

# Secondary Ion Mass Spectrometry Study of Hydrogenated Amorphous Silicon Layer Disintegration upon Rapid (Laser) Annealing

Wolfhard Beyer, Maurice Nuys,\* Gudrun Andrä, Hassan Ali Bosan, Uwe Breuer, Friedhelm Finger, Annett Gawlik, Stefan Haas, Andreas Lambertz, Norbert Nickel, and Jonathan Plentz

We regret to inform our readers that Dr. Wolfhard Beyer has passed away during the review process of this publication.

Double layers of deuterated and hydrogenated amorphous silicon (a-Si:H) on glass are heated in the ambient by scanning with a green (532 nm) continuous wave laser. The hydrogen diffusion length in the laser spot is obtained from the deuterium (D)–hydrogen (H) interdiffusion measured by secondary ion mass spectrometry (SIMS), the temperature in the laser spot is obtained by calculation. Under certain conditions, detachment of the deuterated layer from the hydrogenated layer is observed in the SIMS depth profiles, visible by rising oxygen and carbon signals at the D/H interface attributed to in-diffusion of atmospheric gas species like water vapor, oxygen, and carbon oxide. Stacks involving both undoped and boron-doped a-Si:H films show disintegration. The results suggest that the parameters leading to the disintegration effects are the presence of a plane of reduced material cohesion at the D/H interface, a sizeable H diffusion length and a rather high heating rate. Herein, it is likely considered that the observed layer disintegration process is involved in the peeling of a-Si:H films upon fast heating. Furthermore, the results show that rapid laser heating can be used to detect planes of reduced material cohesion which may compromise the electronic properties of a-Si:H-based stacks.

cells,<sup>[1–3]</sup> silicon heterojunction solar cells,<sup>[4–6]</sup> thin film silicon solar cells on glass,<sup>[7–9]</sup> as well as transistors in large area displays.<sup>[10]</sup> Hydrogen plays a crucial role in these devices as it passivates silicon defects. Of particular importance can be the motion of hydrogen during deposition at elevated temperatures and upon heat treatment. In recent time, interest has increased in details and mechanisms of a-Si:H film disintegration and peeling.<sup>[8,11–13]</sup> These latter effects are known to occur mostly during annealing, in particular involving rapid heating. Related to such disintegration effects may be bubble and pinhole formation due to accumulation of H at interfaces.<sup>[14–16]</sup>

The detachment of H containing silicon alloys and layer stacks upon thermal treatment is crucially problematic for the previously mentioned applications. Hence, it is important to understand the mechanisms

of hydrogen motion to avoid the destruction of the films.

In this article, we study by SIMS depth profiling the disintegration of deuterated and hydrogenated (a-Si:D/a-Si:H) layer structures after annealing by using a continuous wave (CW)

## 1. Introduction

Hydrogenated amorphous silicon (a-Si:H) films are widely used and are of interest for various technologies like thin film solar

W. Beyer, M. Nuys, H. A. Bosan, F. Finger, S. Haas, A. Lambertz  
IEK-5 Photovoltaik  
Forschungszentrum Jülich GmbH  
52425 Jülich, Germany  
E-mail: m.nuys@fz-juelich.de

 The ORCID identification number(s) for the author(s) of this article can be found under <https://doi.org/10.1002/pssa.202200671>.

© 2023 The Authors. physica status solidi (a) applications and materials science published by Wiley-VCH GmbH. This is an open access article under the terms of the Creative Commons Attribution-NonCommercial License, which permits use, distribution and reproduction in any medium, provided the original work is properly cited and is not used for commercial purposes.

DOI: 10.1002/pssa.202200671

G. Andrä, A. Gawlik, J. Plentz  
Research Department Functional Interfaces  
Leibniz Institute of Photonic Technology (Leibniz-IPHT)  
Albert-Einstein-Straße 9, 07745 Jena, Germany

U. Breuer  
ZEA-3 Analytik  
Forschungszentrum Jülich GmbH  
52425 Jülich, Germany

N. Nickel  
Institut für Silizium Photovoltaik  
Helmholtz Zentrum Berlin für Materialien und Energie GmbH  
Kekuléstrasse 5, 12489 Berlin, Germany

laser. The initial phase of detachment of the deuterated layer is detected by the appearance of enhanced SIMS hydrogen, oxygen, and carbon signals, the latter two attributed to atmospheric gas species, at the deuterium–hydrogen interface. The a-Si:D film on top of a-Si:H material allows (by investigation of deuterium (D)-hydrogen (H) interdiffusion) a measurement of the hydrogen diffusion length in the laser spot.<sup>[17]</sup> Focusing on a-Si:H films on glass, the temperature in the laser spot is estimated by calculation, using the laser scanning conditions and the thermal properties of the employed glass substrate, based on previous work.<sup>[17]</sup> We report on layer disintegration effects in relation to H diffusion length, temperature in the laser spot, and heating rate for undoped and boron-doped a-Si:H.

## 2. Results

### 2.1. Stack Disintegration Effects

In **Figure 1**, a series of SIMS depth profiles along with transmitted light images is shown for different laser annealing states of sample L24. Figure 1a–d shows profiles of <sup>1</sup>H (hydrogen), <sup>2</sup>H (hydrogen-2, termed deuterium (D) throughout the article), C (carbon), <sup>18</sup>O (oxygen) as well as silicon. In the as-deposited state (Figure 1a), the a-Si:D layer on top of the a-Si:H layer shows a well-defined interface with a steeply decreasing deuterium (<sup>2</sup>H) concentration at increasing sputtering time. With rising annealing (laser residence) time (Figure 1b,c), the deuterium diffusion length increases, that is, deuterium diffuses further into the a-Si:H material. However, the situation changes abruptly between Figure 1c,d. A reduction of the scan speed from  $\nu = 10\text{--}5\text{ mm s}^{-1}$ , that is, an increase of the laser residence time  $\Delta t = 2r_0/\nu$  from 70 to 140 ms results in a complete change of the depth profiles and a partial detachment of the a-Si:D layer at the a-Si:D/a-Si:H interface, which we term disintegration. It is important to note that the SIMS profiles are measured at positions where the layer stack is not detached. Most notable is the appearance of high carbon and oxygen signals at the a-Si:D/a-Si:H interface, the almost complete mixing of deuterium and hydrogen in the a-Si:H layer and for both D and H in the a-Si:H layer the typical signs of D and H out-diffusion towards the D/H interface and toward the substrate. The out-diffusion of H is confirmed by the overall lower H content in the film compared to Figure 1c. We assign the high carbon and oxygen signals to atmospheric carbon oxide, oxygen, and water molecules penetrating the D/H interface. The absorption of the latter molecules on silicon surfaces at ambient temperatures is known;<sup>[18]</sup> a rapid increase of carbon and oxygen SIMS signals upon exposure to atmosphere was found for porous silicon.<sup>[19]</sup> Note that both oxygen and carbon signals in Figure 1d show reduced values in the range of the a-Si:D layer, that is, carbon and oxygen do not diffuse to the D/H interface passing through the bulk a-Si:D film. Lateral diffusion must be involved. As the SIMS measurements are done under UHV conditions, this gas penetration does not happen during SIMS measurement but must take place earlier. As the laser spot radius used was 0.35 mm, the (lateral) diffusion lengths involved in the heated material must be, thus, of the order mm. Since the

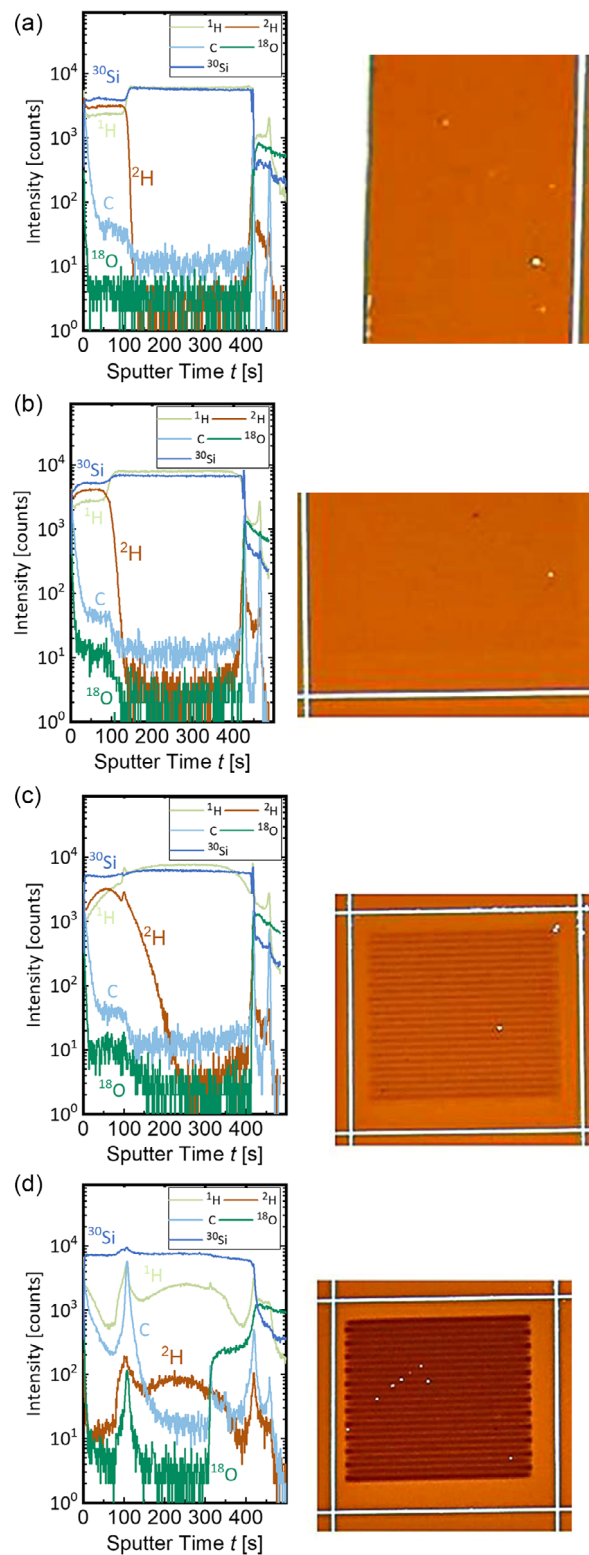


**Figure 1.** SIMS depth profiles of Si, <sup>1</sup>H, <sup>2</sup>H, O, C and transmitted (white) light image a) not annealed (NA), b)  $P = 3\text{ W}$ ,  $\nu = 20\text{ mm s}^{-1}$ ,  $\Delta t = 35\text{ ms}$ , c)  $P = 3\text{ W}$ ,  $\nu = 10\text{ mm s}^{-1}$ ,  $\Delta t = 70\text{ ms}$ , and d)  $P = 3\text{ W}$ ,  $\nu = 5\text{ mm s}^{-1}$ ,  $\Delta t = 140\text{ ms}$ . Laser scanning from glass side. Measured H diffusion lengths: (b) 75 Å, (c) 390 Å, and (d) 2160 Å.

samples investigated are about  $1 \times 1 \text{ cm}^2$  in size, the diffusion length of gas penetration along the interface may be even bigger. As laser scanning was done in ambient and the samples were stored in ambient thereafter, ambient gas penetration may occur during laser scanning and later. Thus, the results of Figure 1 demonstrate that laser scanning under certain conditions causes layer detachment and, thus, stack disintegration.

A comparison of the hydrogen and deuterium ( $^2\text{H}$ ) profiles of Figure 1c,d shows that the stack disintegration (observed for a H diffusion length of  $2160 \text{ \AA}$ , see Figure 1d) is preceded by an H and D ( $^2\text{H}$ ) accumulation at the H/D interface (see Figure 1c) already at much lower H diffusion length of  $390 \text{ \AA}$ . Paired with the H/D interface accumulation in Figure 1c is a slight photodarkening effect in the laser-scanned area (see transmitted light image).<sup>[20]</sup> This photodarkening apparently gets much stronger when stack disintegration occurs (Figure 1d). Almost no photodarkening and no H/D interface accumulation is visible in Figure 1b (H diffusion length  $75 \text{ \AA}$ ).

As is shown in Figure 2, disintegration characteristics can also be found on a stack for fixed laser scanning conditions when the SIMS depth profile is measured at different locations in the scanned area. The photographs of the SIMS crater area show bands of dark and bright appearance. When measured in the bright band of the photograph (Figure 2a) no disintegration is

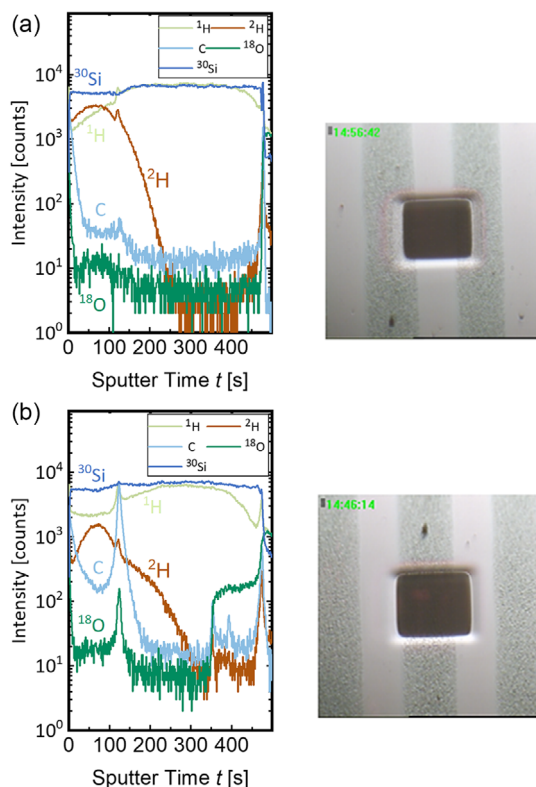


**Figure 2.** SIMS depth profiles of masses  $^1\text{H}$ ,  $^2\text{H}$ , Si, O, and C and photographs of the SIMS crater area of sample L24 for laser treatment conditions:  $P = 3.3 \text{ W}$ , glass side,  $v = 10 \text{ mm s}^{-1}$  (70 ms residence time) in the bright a) and dark b) areas of films. Laser scanning direction in photograph rotated by  $90^\circ$  compared to transmitted light images in Figure 1. SIMS crater dimension:  $300 \times 300 \mu\text{m}$ , laser line offset ( $r_0$ ):  $350 \mu\text{m}$ . Measured H diffusion lengths (a)  $L \approx 360 \text{ \AA}$ , (b)  $L \approx 800 \text{ \AA}$ .

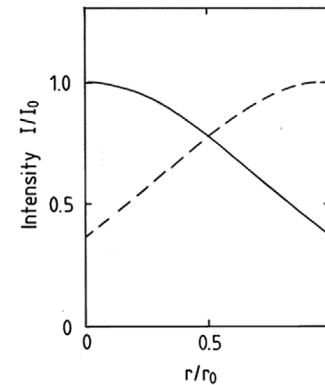


**Figure 3.** Laser intensity profile of two laser lines for present scanning procedure. Maximum intensity  $I/I_0 = 1$  of the first line (full line) at  $r = 0$  and of the second line (dashed line) at  $r = r_0$ . Lowest intensity at  $r/r_0 = 0.5$  with  $I/I_0 = 0.78$ . Laser intensity dependences:  $I = I_0 \exp -(r/r_0)^2$  and  $I = I_0 \exp -((r_0 - r)/r_0)^2$ .

detected. In the area of the dark band of the photograph (Figure 2b), clear disintegration is visible by high carbon and oxygen signals at the D/H interface. This presence of the bands with dark and bright appearance is attributed to the use of Gaussian laser profiles for laser scanning. As the laser lines are the laser spot radius  $r_0$  apart, the laser intensity (and thus the rise of temperature in the laser spot)<sup>[17]</sup> varies perpendicular to the scan direction by as much as about a factor of 0.78 reached at  $r/r_0 = 0.5$ . However, at this latter reduced intensity, the sample is laser-scanned two times. The overlapping of laser intensities is visualized in Figure 3. Common to both cases where the stack disintegration occurs according to the SIMS depth profiles (see Figure 1d and 2b) is a rather high degree of photodarkening<sup>[17,20]</sup> in the transmitted light image, as seen in Figure 1d and 4a. This means a high degree of H out-diffusion.<sup>[17,20]</sup> Apparently, this H out-diffusion which is considered to involve also a shrinkage of the material,<sup>[21]</sup> leads here to a disintegration of the a-Si:D/a-Si:H interface. For the as-deposited material (see Figure 1a), the D/H interface does not show any defect, that is, there is no accumulation of oxygen or carbon at the interface visible in SIMS. Upon moderate annealing (Figure 1b) deuterium and hydrogen diffuse smoothly through this interface.

However, at increasing H/D diffusion length, this interface apparently deteriorates by (first) accumulation of hydrogen (see Figure 1c and 2a) and, at higher H diffusion length, by allowing carbon oxide/oxygen/water molecules to diffuse in laterally

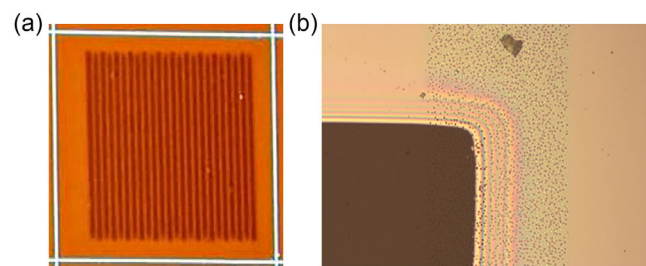


**Figure 4.** a) Transmitted light image of laser scanned area of Figure 2. b) Photograph showing bubble formation in dark band of Figure 2a.

(see Figure 1d and 2b). Also, bubble formation is visible, see Figure 4b showing a magnification of the photograph of Figure 2a. These bubbles apparently form at the film-substrate interface. It is these bubbles which cause the dark bands in the photographs of Figure 2.

Obviously, Figure 1d and 2b show different stages of stack disintegration: Figure 2b seems to be a rather initial one: carbon and oxygen penetrations are already visible but D/H interdiffusion is still possible, yet at reduced concentration. In Figure 1d, in contrast, the D/H interdiffusion apparently is no longer possible and the profiles indicate both H and D out-diffusion from the a-Si:H layer. The complete delamination of the top (a-Si:D) layer is likely prevented by the inhomogeneous line-by-line laser scanning procedure using a Gaussian profile.

The effect of a reduced laser power (2.7 W) is shown in Figure 5a,b. As is seen, despite a rather high H diffusion length ( $L \approx 900 \text{ \AA}$ ) and clearly visible photodarkening in Figure 5b, the (complete) stack disintegration effect is not observed. However, hydrogen interface accumulation is clearly visible in Figure 5b but only barely in Figure 5a ( $L \approx 190 \text{ \AA}$ ). A comparison of the SIMS results of Figure 5b with those of Figure 2b shows that a rather high H diffusion length near 800–900 Å alone does not result in stack disintegration.

Since boron-doping is known to enhance the H diffusion coefficient in a-Si:H<sup>[22,23]</sup> and thus a changed temperature

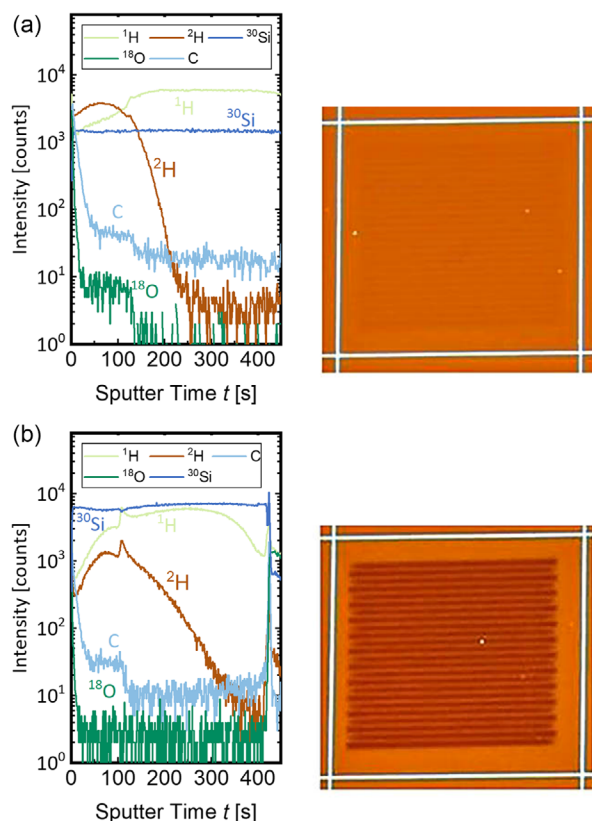


**Figure 5.** SIMS depth profiles of  $^1\text{H}$ ,  $^2\text{H}$ , Si, C, and O and transmitted light images of undoped a-Si:D/a-Si:H (L24) treated with 2.7 W laser power from glass side with speeds  $10 \text{ mm s}^{-1}$  a) and  $5 \text{ mm s}^{-1}$  b). Measured H diffusion lengths in laser spot: (a)  $185 \text{ \AA}$  and (b)  $900 \text{ \AA}$ .

dependence of the H diffusion length is expected, we also studied B-doped a-Si:D/a-Si:H stacks with regard to stack interface disintegration. Typical SIMS depth profiles of our B-doped a-Si:D/a-Si:H samples (not annealed as well as after laser treatment) along with the corresponding transmitted light images are shown in Figure 6. Since trimethylboron was used for boron doping, the samples show in the range of B-doping also a high carbon signal. B is detected as  $\text{SiB}^-$  ion by SIMS. The intended gas phase doping was 1% which was confirmed by B implantation. Thus, we expect within the B-doped material a carbon concentration of the order 3% according to the composition of TMB. The deuterated layer was undoped, that is, electrically n-type while boron doping is known to cause electrically p-type material. The steps in SIMS signal height of  $^2\text{H}$  (D) at the Si:D/Si:C:B:H interface (i.e., the enhancement of  $^2\text{H}$  (D) signals in the B-doped layer, see Figure 6b,d can be attributed to a higher H concentration and thus a higher H solubility in the a-Si:C:B:H compared to the a-Si:D, see Figure 2 in Beyer and Wagner.<sup>[24]</sup> Note that for deuterium diffusion through an interface of different H concentration within amorphous silicon, on both sides of the interface the ratio of  $\text{D}/(\text{H} + \text{D})$  is expected to be the same.<sup>[24]</sup> Such steps in the deuterium concentration measured by SIMS were previously noted also by Street et al.<sup>[23]</sup>

A comparison with undoped material treated by the same laser power ( $P = 2.7 \text{ W}$ ) and laser scan speed ( $\nu = 10 \text{ mm s}^{-1}$ ) (comparing Figure 6c with 5a) shows that indeed in the B-doped material the H diffusion length is clearly higher (about  $700 \text{ \AA}$  in Figure 6c) than in the undoped material ( $L = 185 \text{ \AA}$  in Figure 5a) as expected from the boron doping dependence of H diffusion.<sup>[22,23]</sup> In agreement with an increased photodarkening related to high H out-diffusion,<sup>[20]</sup> Figure 6c also shows an enhanced photodarkening compared to Figure 5a.

As shown in Figure 6, interface disintegration quite similar to the undoped a-Si:H (see Figure 1) occurs in the B-doped stack, however, under different laser treatment conditions. Similar to the undoped a-Si:H, we find also for the B doped stack differences concerning disintegration when measured in the high and low-intensity range of the laser lines. This is seen by comparison of Figure 7a with b (both  $P = 3.3 \text{ W}$ ,  $\nu = 20 \text{ mm s}^{-1}$ ). Clear stack disintegration (visible by the interface oxygen signal) takes only place in the range of the higher laser intensity.

In Figure 8, SIMS depth profiles of the undoped (Figure 8a) and boron-doped (Figure 8b) stacks after 10 and 12 min, respectively, furnace annealing (involving typical heating rates of  $40 \text{ }^\circ\text{C min}^{-1}$ ) are shown. Despite rather high H diffusion lengths ( $L = 880$  and  $1390 \text{ \AA}$ , respectively) no stack disintegration is observed. This result as well as the lacking stack disintegration in Figure 5b demonstrates that a rather high H diffusion length alone does not result in the stack disintegration. Other parameters are apparently involved. In Section 2.3, we shall examine the influence of temperature and heating rate on stack disintegration.

## 2.2. Temperature in the Laser Spot and High-Temperature H Diffusion Coefficients

According to Beyer et al.,<sup>[17]</sup> the temperature in the laser spot can be estimated, based on the heat diffusivity and heat conductance

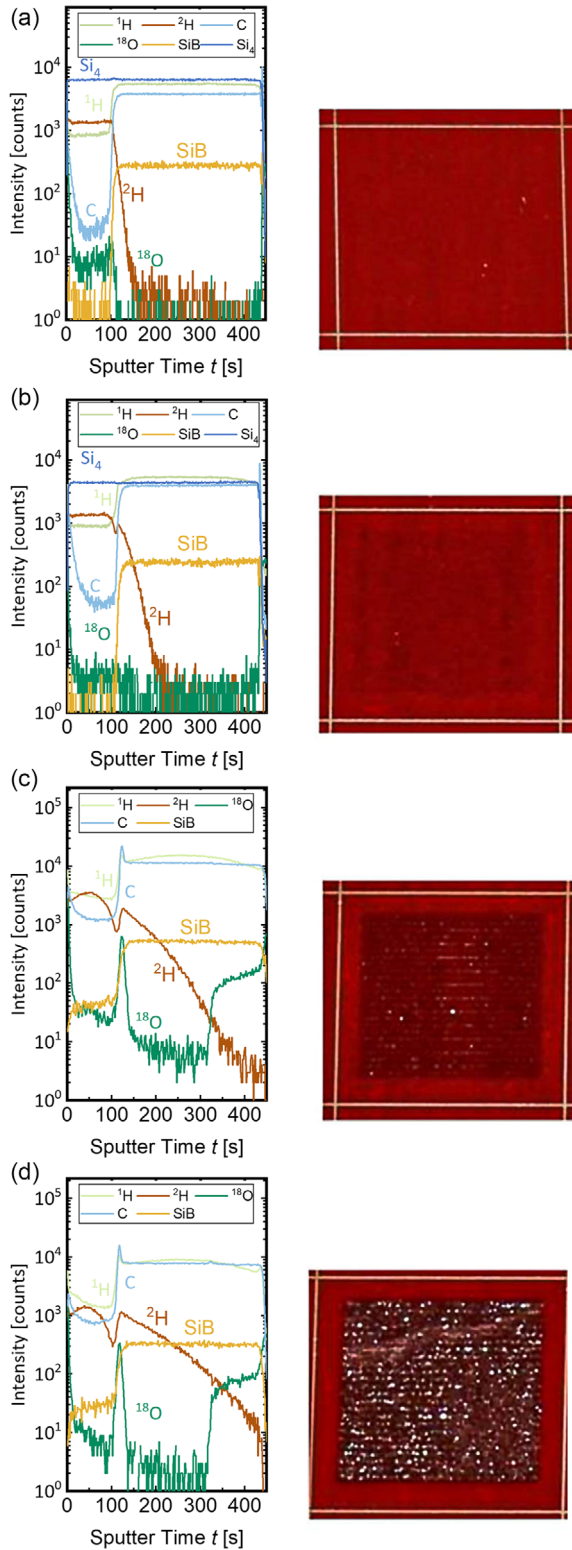


**Figure 6.** SIMS depth profiles of  $^1\text{H}$ ,  $^2\text{H}$  (D), SiB, C, and O and transmitted light images of boron-doped stack L42, laser treated from glass side: a) NA, b)  $P=2.7\text{ W}$ ,  $\nu=20\text{ mm s}^{-1}$ , c)  $P=2.7\text{ W}$ ,  $\nu=10\text{ mm s}^{-1}$ , and d)  $P=2.7\text{ W}$ ,  $\nu=5\text{ mm s}^{-1}$ . Measured H diffusion lengths (b) 200 Å, (c) 700 Å, and (d) 1100 Å.

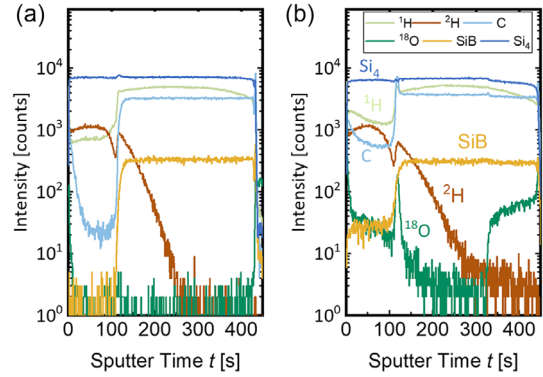


**Figure 7.** SIMS depth profiles of  $^1\text{H}$ ,  $^2\text{H}$ , SiB, Si, C, and O of B-doped a-Si:H (laser treated from glass side at  $P=3.3\text{ W}$ ,  $\nu=20\text{ mm s}^{-1}$ ) outside of laser line a) and within b). Measured H diffusion lengths: (a) 300 Å and (b) 470 Å.

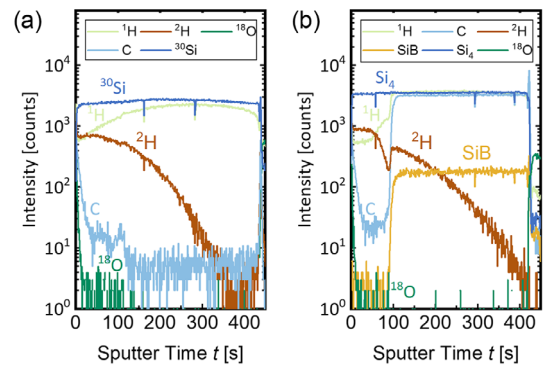


**Figure 8.** SIMS depth profiles of  $^1\text{H}$ ,  $^2\text{H}$ , Si, C, and O in undoped stack L24 a) and of  $^1\text{H}$ ,  $^2\text{H}$ , Si, SiB, C, and O in B-doped stack L42 b) after furnace annealing at (a) 400 °C, 10 min and (b) 350 °C, 12 min. H diffusion lengths from SIMS depth profiles: 880 and 1390 Å, respectively.

of the glass substrate employed, and the laser scanning parameters  $r_0$  and  $\nu$  as well as the laser power  $P^*$  absorbed in the a-Si:H film. For the same laser scanning parameters (and the same substrate material), the same temperature in the laser spot is expected for doped and undoped a-Si:H as long as the refractive index remains unchanged upon doping. Since the H diffusion length  $L$  obtained by the SIMS profiling of the a-Si:D/a-Si:H stacks treated by laser scanning yields the H diffusion coefficient  $D$  by the following equation

$$L = 2(D\Delta t)^{\frac{1}{2}} \quad (1)$$

( $\Delta t$  is the laser residence time = annealing time), the present D–H interdiffusion data allow the measurement of the high-temperature H diffusion coefficient as a function of temperature. One problem of the present laser scanning setup is, however, that a Gaussian laser profile was used, that is, perpendicular to the laser scan direction the absorbed laser power and thus the temperature enhancement varies to some degree, see Figure 3. While we tried to account for this effect by measuring

for the present purpose (i.e., for measuring the H diffusion coefficient) the SIMS depth profiles in the range of highest photodarkening,<sup>[17]</sup> some scatter of data must be expected. In Figure 9a,b, for the undoped a-Si:H samples L12 and L24, the hydrogen diffusion coefficient  $D$  is plotted versus reciprocal temperature  $1/T$  with  $T$  calculated according to Equation (7) in Beyer et al.<sup>[17]</sup> For heat diffusivity and heat/thermal conductivity of the glass substrate, the values  $D_s = 0.00518 \text{ cm}^2 \text{ s}^{-1}$  and  $k = 0.0142 \text{ W cm}^{-1} \text{ }^\circ\text{C}$ , respectively, were used<sup>[17,25]</sup> and for the heat diffusion length in multiples of the laser spot radius  $z = 1$  was assumed.

$$D = 10^{-3} \text{ cm}^2 \text{ s}^{-1} \exp(-1.39 \text{ eV}/kT) \quad (2)$$

The dependence which has been proposed previously on the basis of the Meyer–Neldel rule of H diffusion<sup>[17,26]</sup> is shown in Figure 9a,b as a full line and in Figure 9c as a dashed line. The dashed line in Figure 9a indicates the values for H diffusion coefficient at  $r_0/2$  distant from the maximum laser power (perpendicular to the laser scan direction), accounting for the fact that at this place the stack was scanned twice but ignoring the decrease in laser intensity. As is seen, the experimental results in Figure 9a,b agree very well with Equation (2). Of importance is, furthermore, that these data involve scanning speeds between 1 and 20  $\text{mm s}^{-1}$  demonstrating that the high-temperature H diffusion coefficient turns out to be rather independent of annealing time in agreement with previous work.<sup>[17,26]</sup>

In Figure 9c, the same evaluation as employed for Figure 9a,b is done for the boron-doped sample L42. In the lower temperature range ( $T < 550 \text{ }^\circ\text{C}$ ), a clear enhancement of H diffusion compared to undoped a-Si:H is observed. Below 550  $^\circ\text{C}$ , the H diffusion coefficient agrees with a dependence

$$D = 10^{-3} \text{ cm}^2 \text{ s}^{-1} \exp(-1.09 \text{ eV}/kT) \quad (3)$$

Above about  $T = 550 \text{ }^\circ\text{C}$  (below  $10^3/T \approx 1.3 \text{ K}^{-1}$ ), the values of the H diffusion coefficient  $D$  deviate from Equation (3). Tentatively, we attribute this deviation to H out-diffusion at  $T > 550 \text{ }^\circ\text{C}$  causing a reduced doping effect of the incorporated

boron. All data deviating from the relation of Equation (3) involve H diffusion lengths exceeding about 500  $\text{Å}$ . The results in Figure 9c suggest that at  $T > 700 \text{ }^\circ\text{C}$  ( $1/T < 10^{-3} \text{ K}^{-1}$ ),  $D$  is of the order as in undoped a-Si:H. In this case, the H diffusion length exceeds 1000  $\text{Å}$ , that is, is of the order of sample (stack) thickness (3300  $\text{Å}$ ). Thus, a depletion of hydrogen in the B-doped film is likely and the disappearance of the B doping effect is likely, too, at  $T > 700 \text{ }^\circ\text{C}$  under the present scanning conditions. We note that to our knowledge, the H diffusion coefficient in a-Si:H has not been measured (except noted in our previous publications)<sup>[17,26]</sup> to such high temperatures so far, as a-Si:H typically starts to crystallize near 550  $^\circ\text{C}$  on the time scale of minutes or hours.<sup>[27]</sup> The present measurements are only possible due to the rather short annealing time applied in the laser scanning process. The crystallization temperature of amorphous silicon is known to depend on the annealing time.<sup>[28]</sup>

### 2.3. Influence of Heating Rate

According to Beyer et al.<sup>[17]</sup> and Figure 9, the H diffusion in the investigated temperature range is governed by known Arrhenius dependences, the temperature dependence of the H diffusion length  $L$  for the various scan speeds (and laser residence time  $\Delta t$ ) follows directly by the following equation

$$L = 2 (\Delta t D_0 \exp(-E_D/kT))^{1/2} \quad (4)$$

where  $D_0$  is the H diffusion prefactor,  $E_D$  is the H diffusion energy, and  $k$  is Boltzmann's constant.

In Figure 10a,b,  $L$  is plotted as a function of temperature  $T$  in the laser spot for various scan speeds. For  $D_0$ , we used  $D_0 = 10^{-3} \text{ cm}^2 \text{ s}^{-1}$  (Beyer et al.<sup>[17]</sup> and Figure 9), for  $E_D$ , we used  $E_D = 1.39 \text{ eV}$  (Equation (2), Beyer et al.<sup>[17]</sup> and Figure 9a,b) for undoped a-Si:H and  $E_D = 1.09 \text{ eV}$  (Equation (3), see Figure 9c) for our B-doped a-Si. The open data points indicate stacks without disintegration, the solid data points indicate stacks with disintegration according to SIMS. The results (in particular in Figure 10b) demonstrate that stack disintegration occurs quite systematic with regard to temperature in the laser spot and H

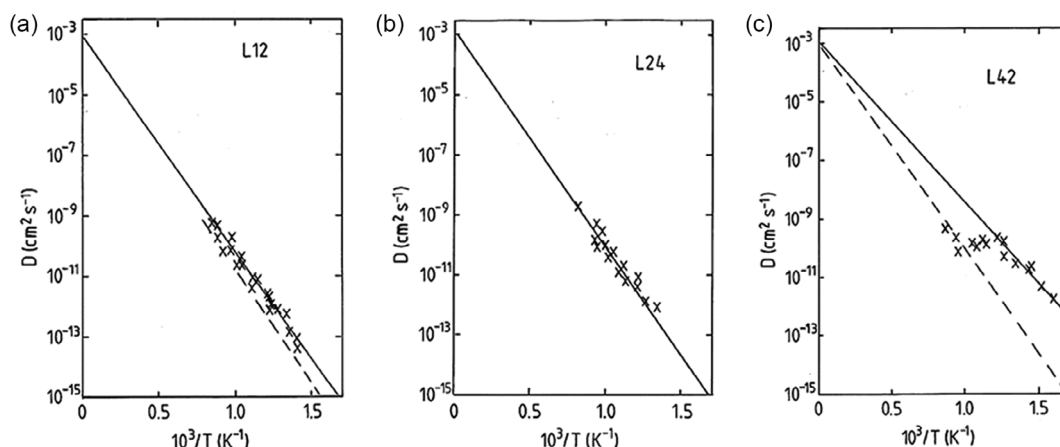


**Figure 9.** Hydrogen diffusion coefficient  $D$  versus  $1/T$  for the undoped a-Si:H sample L12 (dashed line calculated for measurement between laser lines) a), for undoped a-Si:H sample L24 b), and for B-doped a-Si:H sample L42 (dashed line: dependence for undoped a-Si:H) c).  $x$  represent experimentally determined diffusion coefficients from the samples L12, L24, and L42.

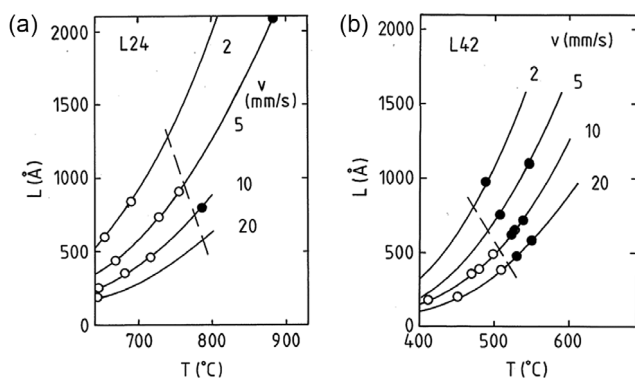


**Figure 10.** Dependence of H diffusion length  $L$  on temperature  $T$  in the laser spot assuming H diffusion coefficient dependences of Figure 9 for a) undoped and b) boron-doped stack for various scan speeds  $v$ . Open circles represent samples without stack disintegration, full dots represent samples with observed disintegration. Dashed line indicates the critical diffusion length versus critical temperature for disintegration.

diffusion length and that the transition (as indicated by the dashed lines) shifts rather strongly with increasing scan speed to lower H diffusion lengths while the temperature in the laser spot is not so much changed. The increased scan speed means an increased heating rate. For sample L24, the heating rate can be estimated (by dividing the temperature increase by the corresponding residence time) to vary from about  $2 \times 10^3 \text{ °C s}^{-1}$  for  $2 \text{ mm s}^{-1}$  scan speed to more than  $10^4 \text{ °C s}^{-1}$  at  $10 \text{ mm s}^{-1}$  scan speed, for sample L42, one can estimate a heating rate of  $1.3 \times 10^3 \text{ °C s}^{-1}$  for the scan speed of  $2 \text{ mm s}^{-1}$  and nearly  $1.5 \times 10^4 \text{ °C s}^{-1}$  at  $20 \text{ mm s}^{-1}$ . Thus, the results show that a higher heating rate favors stack disintegration at lower H diffusion length. This means that the heating rate is in fact an important quantity. A high heating rate tends to cause the stack disintegration likely because of a rapid increase of the H diffusion length with time which may cause, for example, a strongly increasing H pressure within voids or bubbles at the D/H interface.

The results in Figure 10a,b, thus, show a-Si:D/a-Si:H stack disintegration under the present laser scanning conditions at temperatures exceeding about  $450 \text{ °C}$  and for H diffusion lengths exceeding about  $400 \text{ Å}$  for the B-doped material and about  $730 \text{ °C}$  and  $500 \text{ Å}$  for the undoped material, respectively. More in detail, at a scan speed of  $10 \text{ mm s}^{-1}$  ( $70 \text{ ms}$  residence time) and a laser power at or below  $1 \text{ kJ cm}^{-2}$ , disintegration is observed at  $780 \text{ °C}$  and a H diffusion length of about  $750 \text{ Å}$  for undoped and  $500 \text{ °C}$  and about  $500 \text{ Å}$  for our B-doped a-Si:H. Since disintegration is only observed at the D/H interface (and not in the bulk of the a-Si:D or a-Si:H films), apparently a plane of reduced cohesion is required for the disintegration to occur. An a-Si:D/a-Si:H interface of reduced cohesion may be caused by surface reconstruction of the a-Si:H film taking place before the a-Si:D film is deposited. Nucleation effects<sup>[29]</sup> in the initial phase of a-Si:D growth may be involved. Residual water or oxygen adsorption may also play a role despite a vacuum of  $<7 \times 10^{-8} \text{ mbar}$  in the deposition system during process gas (silane to deuteriosilane) change. The interface between a-Si:D and a-Si:C:B:H is likely of even poorer quality

as a transfer from one deposition chamber to the other was involved. We consider it likely that voids/bubbles at such planes are present already after deposition or they form when at enhanced temperature hydrogen starts to diffuse. Upon heating, molecular hydrogen/deuterium will desorb into such bubbles and eventually an enhancement of bubble concentration/size will occur leading to disintegration effects. The difference between undoped and boron-doped a-Si:H is attributed to the difference of the temperature-dependent H diffusion coefficient.<sup>[22,23]</sup> We note that such a disintegration mechanism may not be confined to a-Si:D/a-Si:H layer interfaces and may well occur within entirely amorphous a-Si:H material at planes defined by high strain.<sup>[11]</sup> These effects need to be considered when a-Si:H films are annealed, in particular, at high heating rates. Our results show, furthermore, that a high H diffusion length alone does not necessarily lead to disintegration, see Figure 5b and 8. Apparently, a high heating rate is also required.

### 3. Discussion

The primary results of this work are 1) the finding of heating-induced disintegration of a-Si:D/a-Si:H stacks; and 2) the measurement of high-temperature H diffusion in boron-doped a-Si:H: The hydrogen diffusion-related disintegration of a-Si:H films is of importance for any annealing procedures of a-Si:H, like, for example, the dehydrogenation of a-Si:H for the purpose of precursor layers for solid or liquid phase crystallization. The present results suggest that primarily the H diffusion length is of critical importance but also the temperature, the heating rate, and the presence of planes of reduced connectivity. Rapid annealing of layer structures involving hydrogenated amorphous/microcrystalline silicon materials may be affected by such disintegration. We think that this disintegration effect can be considered to serve as a model for the peeling of a-Si:H films which may be of importance, for example, for the fabrication of silicon on glass devices like solar cells.<sup>[11]</sup> This effect is observed for intrinsic as well as B-doped a-Si:H films.

With regard to interfaces, the results show that our a-Si:H-based layer structures L24 and L42 have weak interfaces. Further work may show if by refined film deposition techniques such interfaces (“planes of poor cohesion”) between (e.g.) intrinsic–intrinsic (i–i), p-doped–intrinsic (p–i), and n-doped–intrinsic (n–i) material can be avoided. Indeed, sample L12 did not show the pronounced stack disintegration as visible for the samples L24 and L42. However, hydrogen accumulation at the D/H interface which must be considered as a precursor to disintegration was observed also for sample L12 at high temperature and high H diffusion length, see Figure 2b in Beyer et al.<sup>[17]</sup> Thus, the present experiment of laser scanning paired with SIMS profiling may serve to detect such weak interfaces. The property of such weak interface is apparently that upon rapid heating, hydrogen atoms and/or molecules accumulate there. An increased concentration of weak Si–Si bonds or voids is likely involved which may compromise the electronic properties in this range, with consequences for devices.

We note that interfaces of the type present in this article are quite common in, for example, thin film silicon as well as Si heterojunction solar cell technology. The reduced material cohesion

observed here may, for example, inhibit solar cell performance. Although a-Si:H based devices are often deposited on textured (rough) substrates so that peeling even at high heating rate is unlikely, the effects of growth-related reduced material cohesion (increased concentration of voids) may still be present in particular at certain interfaces like p-i or n-i, and result in electronic defects. In addition, the diffusion behaviors of intrinsic and B-doped a-Si:H films are investigated. While for the intrinsic samples (L24 and L12), the diffusion behavior is confirmed to be independent of the annealing time, the diffusion of the B-doped film (L42) differs from the known diffusion characteristic. For  $T < 500\text{ }^\circ\text{C}$ , the H diffusion is considerably enhanced while for high temperatures ( $T > 700\text{ }^\circ\text{C}$ ) a diffusion coefficient like those from undoped films are observed. This result shows that the doping effect by boron on H diffusion is present up to about  $550\text{ }^\circ\text{C}$ .

## 4. Conclusion

Interfaces in a-Si:H layer stacks are found to be sensitive to disintegration/layer detachment upon rapid heating like applied by laser scanning. The results suggest that these interfaces can involve planes of reduced cohesion where diffusing hydrogen can accumulate in voids or bubbles and thus cause stack disintegration/layer detachment and peeling. This effect is observed independent of the doping of the involved films. Important parameters are the H diffusion length, the temperature, and the heating rate. The results show that such planes of reduced cohesion which may have compromising electronic consequences can be detected by rapid laser heating along with SIMS depth profiling.

Note that such planes of reduced cohesion and the accumulation of hydrogen at these interfaces might also be a crucial for the stability upon (rapid) annealing of layer stacks including other silicon alloys such oxides, nitrides, and carbides.

## 5. Experimental Section

The investigated films were deposited at Forschungszentrum Jülich by radio frequency (rf, 13.56 MHz) glow discharge. As a substrate, Corning Eagle XG<sup>[25]</sup> (borosilicate) glass plates of dimension  $10 \times 10\text{ cm}^2$  were used. The deposition temperature was about  $185\text{ }^\circ\text{C}$ . The laser heating of the undoped stacks (termed L12 and L24) was already discussed previously.<sup>[17]</sup> In these cases, the a-Si:H and a-Si:D layers were deposited in same chamber. Flows of SiH<sub>4</sub>, SiD<sub>4</sub> as well as hydrogen were used. In detail, for the a-Si:H films a flow of 10 sccm SiH<sub>4</sub> and a flow of 90 sccm H<sub>2</sub> was employed, the rf power was 5 W and the pressure was 4 mbar. The electrode distance was 11 mm, the electrode area was  $156\text{ cm}^2$ . For the a-Si:D films, the same conditions were used except that the SiH<sub>4</sub> flow was exchanged by a SiD<sub>4</sub> flow. The change from SiH<sub>4</sub> flow to SiD<sub>4</sub> flow involved just the turning off the rf power and shutting off the flow of SiH<sub>4</sub>/H<sub>2</sub>, the pumping of the chamber to  $< 7 \times 10^{-8}$  mbar and then the turning on of the SiD<sub>4</sub>/H<sub>2</sub> flow and the rf power. For L24, thickness of the stack (a-Si:H/a-Si:D) was approximately  $0.35\text{ }\mu\text{m}$  and the a-Si:D layer was approximately  $0.07\text{ }\mu\text{m}$  thick. For L12, the corresponding parameters were  $0.74$  and  $0.08\text{ }\mu\text{m}$ . Hydrogenated amorphous silicon deposited under the applied conditions had been used in thin-film silicon solar cells.<sup>[30]</sup> Previous work showed that such material was rather dense (compact) with the diffusion of hydrogen predominantly by atoms and not by molecules.<sup>[21,31]</sup>

For the deposition of the boron-doped stack (termed L42), trimethylboron (trimethylborane, TMB) was used as the boron carrier gas. Flows of

12 sccm SiH<sub>4</sub>, 110 sccm H<sub>2</sub>, and 12 sccm of 1% TMB in He (i.e., 1% B in silane gas flow) were applied. The gas pressure was 1.06 mbar, the rf power was 3 W, and the electrode distance was 20 mm. After the deposition of this a-Si:C:B:H layer (which we term also boron-doped a-Si:H), the substrate was transferred to another chamber for the deposition of the (undoped) a-Si:D layer. The conditions used here were the same as for samples L12 and L24, namely, 10 sccm SiD<sub>4</sub> and 90 sccm H<sub>2</sub>, 5 W, 4 mbar, electrode distance 11 mm. Thickness of the stack was approximately  $0.33\text{ }\mu\text{m}$  and the a-Si:D layer was approximately  $0.07\text{ }\mu\text{m}$  thick. The transfer time (in Ultra-high vacuum (UHV)) between the chambers was  $< 3$  min.

Laser scanning was done at Leibniz IPHT in Jena using a Coherent Verdi laser with a wavelength of 532 nm and a nominal maximum optical power of 6.5 W. This laser light was almost fully absorbed in (doped and undoped) a-Si:H at a depth of about  $0.1\text{ }\mu\text{m}$ . A circular Gaussian laser spot of the radius  $r_0 = 0.35\text{ mm}$  (defined by  $1/e$  reduction of the laser intensity) was scanned over fields of about  $9 \times 9\text{ mm}$  at a scan speed between 2 and  $20\text{ mm s}^{-1}$  and a line offset of  $0.35\text{ mm}$  ( $=r_0$ ). The scan speed  $v$  corresponded to the laser residence time  $\Delta t = 2r_0/v$ <sup>[17]</sup> which was considered as the material annealing time in the laser scanning process. Note, that increased scan speed translates into increased heating rates. Applied in the present article were laser energies at and below 3.5 W corresponding to energy flows near and below  $1\text{ kJ cm}^{-2}\text{ s}^{-1}$ . Laser scanning for samples L24 and L42 was done both from the glass and film sides, for sample L12 only from the glass side. Transmitted light images (using white light for illumination) of the undoped stacks L12 and L24 are shown in Beyer et al.<sup>[17]</sup>

For measuring the deuterium-hydrogen interdiffusion after laser scanning, secondary ion mass spectrometry (SIMS) was used. Time of flight instruments (TOFSIMS-IV, and TOFSIMS-V, Iontof GmbH, Münster, Germany) at Forschungszentrum Jülich was employed. An area of  $300 \times 300\text{ }\mu\text{m}^2$  was (typically) sputtered (using a cesium ion beam) and an area of about  $80 \times 80\text{ }\mu\text{m}^2$  was measured using (usually) a Bi<sub>3</sub> ion beam. The depth of the SIMS sputtering craters was determined by a Veeco Dektak 150 profilometer. By fitting the D/(D + H) signals versus depth with complementary error functions, the deuterium/hydrogen diffusion lengths  $L$  are obtained.<sup>[32]</sup>

## Acknowledgements

The authors would like to dedicate this manuscript to the memory of the late Dr. Wolfhard Beyer who passed away during the review process. Wolfhard Beyer was a highly respected scientist who had a long and distinguished career in the field of amorphous semiconductors. This paper represents the final manuscript that he wrote by himself, and it is a testament to his dedication and passion for science. Despite his advancing age, he remained committed to advancing the field and sharing his knowledge with others. His contributions to the understanding of amorphous silicon and its alloys are immeasurable, and he will be deeply missed by his colleagues, friends, and family. We have lost an outstanding scientist, a patient teacher, and a kind-hearted person. We will always remember him in this way. Part of the present work was funded by the BMU/BMWi Globe Si (Jülich/Berlin/Jena) (0335446) Project. The authors at Leibniz IPHT acknowledge the financial support by Federal Ministry for Economic Affairs and Energy within the project FUN (03EE1022C). Technical support by J. Bergmann, D. Lennartz, S. Moll, T. Schmidt is gratefully acknowledged.

Open Access funding enabled and organized by Projekt DEAL.

## Conflict of Interest

The authors declare no conflict of interest.

## Data Availability Statement

The data that support the findings of this study are available from the corresponding author upon reasonable request.

## Keywords

amorphous silicon, annealing, interfaces, thermal stability

Received: September 27, 2022

Revised: March 8, 2023

Published online: May 9, 2023

- [1] A. V. Shah, H. Schade, M. Vanecek, J. Meier, E. Vallat-Sauvain, N. Wyrsh, U. Kroll, C. Droz, J. Bailat, *Prog. Photovoltaics Res. Appl.* **2004**, *12*, 113.
- [2] D. E. Carlson, C. R. Wronski, *Appl. Phys. Lett.* **1976**, *28*, 671.
- [3] J. Plentz, G. Andr , T. Pliwischkies, U. Br ckner, B. Eisenhawer, F. Falk, *Mater. Sci. Eng., B* **2016**, *204*, 34.
- [4] S. DeWolf, A. Descoedres, Z. C. Holman, C. Ballif, *Green* **2012**, *2*, 7.
- [5] K. Masuko, M. Shigematsu, T. Hashiguchi, D. Fujishima, M. Kai, N. Yoshimura, T. Yamaguchi, Y. Ichihashi, T. Mishima, N. Matsubara, T. Yamanishi, T. Takahama, M. Taguchi, E. Maruyama, S. Okamoto, *IEEE J. Photovoltaics* **2014**, *4*, 1433.
- [6] I. Mart n, G. L pez, J. Plentz, C. Jin, P. Ortega, C. Voz, J. Puigdollers, A. Gawlik, G. Jia, G. Andr , *Phys. Status Solidi A* **2019**, *216*, 1900393.
- [7] M. A. Green, P.-A. Basore, N. Chang, D. Clugston, R. Egan, R. Evans, D. Hogg, S. Jarnason, M. Keevers, P. Lasswell, J. O'Sullivan, U. Schubert, A. Turner, S. R. Wenham, T. Young, *Sol. Energy* **2004**, *77*, 857.
- [8] O. Gabriel, T. Frijnts, S. Calnan, S. Ring, S. Kirner, A. Opitz, I. Rothert, H. Rhein, M. Zelt, K. Bhatti, J. H. Zollondz, A. Heidelberg, J. Haschke, D. Amkreutz, S. Gall, F. Friedrich, B. Stannowski, B. Rech, R. Schlatmann, *IEEE J. Photovoltaics* **2014**, *4*, 1343.
- [9] G. Jia, A. Gawlik, J. Plentz, G. Andr , *Sol. Energy Mater. Sol. Cells* **2017**, *167*, 102.
- [10] Y. Kuo, *Electrochem. Soc. Interface* **2013**, *22*, 55.
- [11] H. A. Bosan, W. Beyer, U. Breuer, F. Finger, N. Hambach, M. Nuys, F. Pennartz, D. Amkreutz, S. Haas, *Phys. Status Solidi A* **2021**, *218*, 2000435.
- [12] Z. Said-Bacar, P. Prathap, C. Cayron, F. Mermet, Y. Leroy, F. Antoni, A. Slaoui, E. Fogarassy, *Appl. Surf. Sci.* **2012**, *258*, 9359.
- [13] N. Pham, Y. Djeridane, A. Abramov, A. Hadjadj, P. Roca I Cabarrocas, *Mater. Sci. Eng., B* **2009**, *159–160*, 27.
- [14] H. R. Shanks, L. Ley, *J. Appl. Phys.* **1981**, *52*, 811.
- [15] S. Jafari, J. Steffens, M. Wendt, B. Terheiden, S. Meyer, D. Lausch, *Phys. Status Solidi B* **2020**, *257*, 2000097.
- [16] S. Choi, O. Kwon, K. H. Min, M. S. Jeong, K. T. Jeong, M. G. Kang, S. Park, K. K. Hong, H. Song, K. Kim, *Sci. Rep.* **2020**, *10*, 9672.
- [17] W. Beyer, G. Andr , J. Bergmann, U. Breuer, F. Finger, A. Gawlik, S. Haas, A. Lambertz, F. C. Maier, N. H. Nickel, U. Zastrow, *J. Appl. Phys.* **2018**, *124*, 153103.
- [18] J. T. Law, E. E. Francois, *J. Phys. Chem.* **1956**, *60*, 353.
- [19] L. T. Canham, M. R. Houlton, W. Y. Leong, C. Pickering, J. M. Keen, *J. Appl. Phys.* **1991**, *70*, 422.
- [20] D. L. Staebler, *J. Appl. Phys.* **1979**, *50*, 3648.
- [21] W. Beyer, in *Semiconductors and Semimetals* (Ed: N. H. Nickel), Vol. 61, Academic Press, San Diego, CA **1999**, pp. 165–239.
- [22] W. Beyer, H. Wagner, H. Mell, *Solid State Commun.* **1981**, *39*, 375.
- [23] R. A. Street, C. C. Tsai, J. Kakalios, W. B. Jackson, *Philos. Mag. B* **1987**, *56*, 305.
- [24] W. Beyer, H. Wagner, *Proc. MRS Symp.* **1994**, *336*, 323.
- [25] Corning XG Data Sheet, <https://valleydesign.com/Datasheets/Corning-Eagle-XG-glass.pdf> (accessed: March 2022).
- [26] W. Beyer, J. Bergmann, U. Breuer, F. Finger, A. Lambertz, T. Merdzhanova, N. H. Nickel, F. Pennartz, T. Schmidt, U. Zastrow, *MRS Proc.* **2015**, *1770*, 1.
- [27] J. Plentz, T. Schmidt, A. Gawlik, J. Bergmann, G. Andr , D. Hauschild, V. Lissotschenko, *Phys. Status Solidi A* **2017**, *214*, 1600882.
- [28] N. A. Blum, C. Feldman, *J. Non-Cryst. Solids* **1972**, *11*, 242.
- [29] R. W. Collins, in *Amorphous Silicon and Related Materials* (Ed: H. Fritzsche), World Scientific, Singapore **1989**, pp. 1003–1044.
- [30] A. Lambertz, F. Finger, R. E. I. Schropp, U. Rau, V. Smirnov, *Prog. Photovoltaics Res. Appl.* **2015**, *23*, 939.
- [31] W. Beyer, *Sol. Energy Mater. Sol. Cells* **2003**, *78*, 235.
- [32] D. E. Carlson, C. W. Magee, *Appl. Phys. Lett.* **1978**, *33*, 81.